Sensors and Actuators B 211 (2015) 164–169

Contents lists available at ScienceDirect

Sensors and Actuators B: Chemical

journal homepage: www.elsevier.com/locate/snb

A highly specific pyrene-based fluorescent probe for hypochlorite and its application in cell imaging

Libin Zang[a,b], Chunshuang Liang[a], Ying Wang[a], Wenhuan Bu[c], Hongchen Sun[c], Shimei Jiang[a,*]

[a] State Key Laboratory of Supramolecular Structure and Materials, Jilin University, 2699 Qianjin Avenue, Changchun 130012, PR China
[b] College of Geo-Exploration Science and Technology, Jilin University, Changchun 130026, PR China
[c] Department of Oral Pathology, School and Hospital of stomatology, Jilin University, 1500 Qinghua Road, Changchun 130021, PR China

ARTICLE INFO

Article history:
Received 14 July 2014
Received in revised form 16 January 2015
Accepted 19 January 2015
Available online 28 January 2015

Keywords:
Fluorescent probe
Pyrene
Phenylhydrazone
Hypochlorite

ABSTRACT

A fluorescent probe, 1-pyrenecarboxaldehyde, 2-phenylhydrazone (**1**), has been successfully developed for the detection of hypochlorite on the basis of a specific reaction with phenylhydrazone. The design strategy for the probe is based on the strong quenching effect of electron-donor phenylhydrazone on pyrene fluorescence via the photoinduced electron transfer process, and is accomplished through constructing the conjugated molecule by using a cleavable C=N bond as a linker. This probe reacts selectively with hypochlorite over other ions and reactive oxygen species (ROS), accompanied by 42.6-fold fluorescence enhancement. Biological imaging studies using living cells (HeLa cells) to detect hypochlorite are successfully demonstrated.

1. Introduction

Hypochlorite (OCl^-) has been extensively used as a bleaching agent and disinfectant in our daily lives [1]. Its protonated form, hypochlorous acid (HOCl), is one of the biologically important reactive oxygen species (ROS). In living organisms, hypochlorite is synthesized from hydrogen peroxide and chloride ions in a chemical reaction catalyzed by the enzyme myeloperoxidase (MPO), which is localized mainly in leukocytes, including neutrophils, macrophages, and monocytes [2,3]. However, excessive or misplaced production of hypochlorite can lead to tissue damage and diseases, such as atherosclerosis [4], arthritis [5], and cancers [6]. Therefore, estimating the amount of hypochlorite (OCl^-) in drinking water and organism is especially significant. Toward this end, a number of methods, such as colorimetric [7–11], fluorescent [12,13], electrochemical [14] and chromatographic [15] have been proposed. However, fluorescent sensing is advantageous because of it causes less cell damage while displaying, high time and spatial resolution capabilities in visualizing analytes of biological interest in living cells [16–18]. Recently, a number of fluorescent probes for HOCl/OCl^- sensing have been reported through modification of common fluorophores such as rhodamine [19–25], BODIPY [26,27], and fluorescein [28] with HOCl/OCl^- reactive groups. In addition, Lin et al. [29] successfully design several ratiometric fluorescent probes for hypochlorite based on deoximation reaction, intramolecular charge transfer (ICT) [30] and fluorescence resonance energy transfer (FRET) [31], respectively. However, fluorescent probes that show fluorescence "turn-on" response are still a little scarce, and those of higher sensitivity and selectivity for OCl^- are still required for biological imaging applications [32]. Besides, pyrene-based chemical and biological sensors have attracted intense attention due to their emission wavelengths in the visible region as well as a high fluorescence quantum yield, and their selective emission response to specific analytes. However, as a common fluorophore, pyrene has not yet been used in the development of hypochlorite fluorescent probes to the best of our knowledge.

To rationally design a new fluorescent probe for OCl^-, a selective chemical reaction mediated by OCl^- is highly sought. It is known that OCl^- is a strong oxidant. So, a specific probe with reducibility may be oxidized by OCl^- selectively. In addition, the emissions need be modulated simultaneously. With these in mind, we constructed 1-pyrenecarboxaldehyde, 2-phenylhydrazone (**1**) as a candidate for fluorescent OCl^- probe. The selection of compound **1** is due to the consideration that **1** has reducibility owing to its phenylhydrazone group which may be oxidized by OCl^-. Meanwhile, compound **1** is essentially non-fluorescent because the conjugate phenylhydrazone group (as an electron-donor) has a strong quenching effect on

* Corresponding author. Tel.: +86 431 85168474; fax: +86 431 85193421.
E-mail address: smjiang@jlu.edu.cn (S. Jiang).

http://dx.doi.org/10.1016/j.snb.2015.01.046
0925-4005/

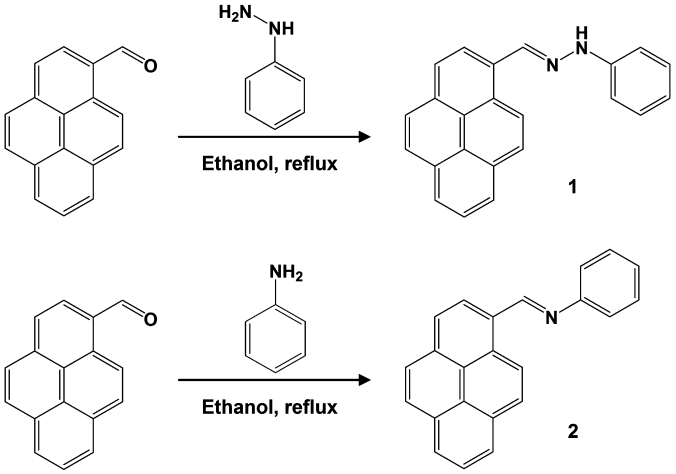

Scheme 1. Synthesis of compounds **1** and **2**.

pyrene fluorescence via the photoinduced electron transfer (PET) process. Thus, compound **1** may act as a "turn on" fluorescent probe for OCl^-.

Accordingly, the spectroscopic properties of **1** reveal that the phenylhydrazone group in the probe can be selectively cleaved by OCl^- instead of the other ions and reactive oxygen species, concomitant with a great increase in fluorescence. Moreover, the probe is cell membrane permeable, and its applicability has been demonstrated for fluorescence imaging of OCl^- in the human cervical cancer cells (HeLa cells).

2. Experimental

2.1. Materials and measurements

All the materials for synthesis and spectra were purchased from commercial suppliers and used without further purification. Hypochlorite was prepared from the 10 wt% commercial sodium hypochlorite solution, and the concentration of it was titrated according to iodometry.

The UV–vis absorption spectra were taken on a Shimadzu 3100 UV–VIS–NIR recording spectrophotometer using a 2 nm slit width. The fluorescence spectra were determined with a Shimadzu RF-5301 PC spectrofluorophotometer using 3 nm input and 1.5 nm output width (excitation at 355 nm). Unless otherwise noted, the spectra were measured in 0.01 M $Na_2B_4O_7$ buffer (pH = 9.18)/ethanol (v/v, 1:4) after the mixtures being equilibrated for 30 min at room temperature. The quantum yield was measured at room temperature referenced to quinine sulfate in aqueous solution of sulfuric acid [33]. ^{1}H NMR (nuclear magnetic resonance) data (tetramethylsilane as a reference) were recorded on a Bruker Ultra Shield 500 MHz spectrometer. The mass spectra were recorded on a liquid chromatograph–mass spectrometer (LC–MS) with UV/ELSD (Ultraviolet Detector/Evaporative Light-scattering Detector). Elemental analyses were performed by vario MICRO cube elementar.

2.2. Synthesis

Compounds **1** and **2** were conveniently obtained by aldehyde-ammonia condensation reaction (Scheme 1). Their structures were characterized by mass spectrometry (MS), elemental analysis, and ^{1}H NMR (see Supplementary data, Figs. S1 and S2).

2.2.1. 1-Pyrenecarboxaldehyde, 2-phenylhydrazone (*1*)

A 0.1135 g (0.49 mmol) sample of 1-pyrenecarboxaldehyde was suspended in 10 mL of ethanol, to which 0.1179 g (1.09 mmol) of phenylhydrazine was added, and the mixture was refluxed for 3 h. During the reaction, a yellow solid precipitate appeared. After the reaction, the system was cooled in the ice bath. The precipitate was then filtered and washed with 15 mL of cold ethanol, affording product **1** as a yellow powder (0.1194 g, 76%). ^{1}H NMR (500 MHz, DMSO): 6.825 (t, J = 7.0 Hz, 1H), 7.217 (d, J = 7.5 Hz, 2H), 7.306 (t, J = 7.0 Hz, 2H), 8.088 (t, J = 7.5 Hz, 1H), 8.184 (s, 2H), 8.301 (d, J = 8.0 Hz, 4H), 8.569 (d, J = 8.0 Hz, 1H), 8.763 (d, J = 9.5 Hz, 1H), 8.912 (s, 1H), 10.677 (s, 1H, NH). Elemental analysis calculated for $C_{23}H_{16}N_2$: C, 86.22; H, 5.03; N, 8.74%. Found: C, 85.91, H, 5.067; N, 8.75%. MS: 320.9 [**1** + H^+].

2.2.2. (E)-N-(pyren-1-ylmethylene)benzenamine (*2*)

A 0.2000 g (0.87 mmol) sample of 1-pyrenecarboxaldehyde was suspended in 15 mL of ethanol, to which 1 mL (11.96 mmol) of phenylamine was added, and the mixture was refluxed for 4 h. After the reaction, the system was cooled in the ice bath. The precipitate was then filtered and washed with 15 mL of cold ethanol, obtaining the yellow product (0.1622 g, 61%). ^{1}H NMR (500 MHz, DMSO): 7.33 (m, 1H), 7.502 (m, 4H), 8.153 (t, J = 7.5 Hz, 1H), 8.261 (d, J = 9.0 Hz, 1H), 8.321 (d, J = 9.0 Hz 1H), 8.404 (m, 4H), 8.791 (d, J = 8.0 Hz, 1H), 9.279 (d, J = 9.5 Hz, 1H), 9.647 (s, 1H). Elemental analysis calculated for $C_{23}H_{15}N$: C, 90.46; H, 4.95; N, 4.59%. Found: C, 90.00, H, 4.996; N, 4.60%.

2.3. Preparation of reactive oxygen/nitrogen species (ROS/RNS)

The stock H_2O_2 (30%) solution was purchased from commercial suppliers and the concentration of H_2O_2 was titrated according to iodometry.

2.3.1. Preparation of ROO·

ROO· was generated from 2,2′-azobis(2-amidinopropane)dihydrochloride. AAPH (2,2′-azobis(2-amidinopropane) dihydrochloride) was added to deionized water and then stirred at room temperature for 1 h [13].

2.3.2. Preparation of NO·

Nitric oxide radical was generated from SNP (sodium nitroferricyanide (III) dihydrate). SNP was added to deionized water and then stirred for 1 h at room temperature [23].

2.3.3. Preparation of ·OH

Hydroxyl radical was generated by the Fenton reaction. To prepare ·OH solution, ferrous sulfate was added in the presence of 50 μM of H_2O_2 [26].

2.4. General procedure of cell imaging

The human cervical cancer cells (HeLa cells) were cultured by the previous method [34]. All of the sensor **1** solutions contained 50% ethanol (v/v, final concentration) as co-solvent. The concentration of **1** was 50 μM. Images were analyzed using an Olympus IX83 fluorescence microscope.

3. Results and discussion

3.1. Absorption and fluorescence spectra studies

The absorption spectra of solutions containing **1** and varying concentrations of OCl^- were shown in Fig. 1. Probe **1** alone had an absorption peak in the visible region (red curve) at 407 nm. As the concentration of OCl^- increased in a stepwise fashion, the absorption intensity of **1** at 407 nm gradually decreased. Meanwhile, two new absorption peaks appeared at 343 nm as well as 328 nm, and their intensity gradually increased. These spectral changes could